

Coating/substrate interaction in elastomer-steel bilayer armor

CB Giller, RM Gamache, KJ Wahl, AP Saab and CM Roland

Abstract

The properties of steel substrates coated with soft polymers were characterized, in order to assess their connection to ballistic properties. An impact-induced viscoelastic phase change of the polymer effects large energy dissipation, while also spreading the force over a wider area, which reduces the impact pressure. Both effects enhance the performance, as directly measured and seen from strain measurements on the substrate taken during ballistic tests. The contribution of the front-surface polymer to impact performance is increased for harder substrates, indicating a coupling of the layers related to impedance mismatching. Since this effect is very local, the phenomenon can be exploited by surface-hardening of the steel.

Keywords

Ballistics, armor, elastomer coatings, phase transition, surface-hardening

Introduction

There are three main requirements for armor: (i) provide sufficient stopping power for the perceived threat (e.g. ball or armor-piercing (AP) bullets, bomb fragments, etc.); (ii) for mobile and body armor applications, minimize weight (or “areal density”—the weight per unit area); (iii) low system cost, which includes materials and fabrication. Generally these three requirements cannot all be optimized, so that armor design invariably entails some compromise. A recent development in ballistic protection is the use of soft polymers on the front (strike) face of armor.^{1,2} This approach has the potential to address all three requirements, since polymers are lighter and (sometimes) cheaper than steel. The key is obtaining improved ballistic properties. In recent work we have shown that certain elastomeric polymers, characterized by high, but sub-ambient, glass transition temperatures, significantly increase the resistance to penetration of steel and other hard substrates.³ Two operative mechanisms have been identified. First is a rapid compression of the rubber coating by the projectile, at strain rates on the order of the frequency of the local segmental dynamics of the polymer, causing large energy absorption.⁴ Second is a reversible change of the material to a glassy state, which increases the modulus by about three orders of magnitude. This transient hardening

causes lateral spreading of the impact force, reducing the impact pressure. Work to date has shown that a thin (few mm) rubber coating can substantially increase the stopping power of armor, or maintain performance with twofold or greater reductions in areal density.⁴

In this work we report ballistic data for fragment-simulating projectiles (fsp), of polymer-coated substrates encompassing a range of areal densities. The elastomer coatings function best for blunt rounds (fsp and ball ammunition, the latter a colloquial term for bullet with round or flat ogives). AP bullets, having a sharp tip, tend to cut the elastomer, reducing its effectiveness. We describe measurements of the substrate deformation, intended to corroborate the lateral spreading of the impact force inferred from the penetration hole size. We also report an unexpected interaction of the polymer coating and steel, whereby harder substrate surfaces enhance the contribution of the elastomer to the ballistic performance.

Chemistry Division, Naval Research Laboratory, USA

Corresponding author:

CM Roland, Chemistry Division, Code 6105, Naval Research Laboratory, Washington, DC 20375-5342, USA.
Email: roland@nrl.navy.mil

Experimental

Ballistic tests followed Mil-Std-662F, using a 5 foot long, rifled Mann barrel. The latter is a heavy-walled test barrel designed for accuracy. The barrel was mounted with concentric rings and maintained in a fixed position during testing. The gun was remotely triggered electrically, using percussion-primed cartridges initiated by a solenoid-driven striker. The projectiles were 0.50 cal fsp, weighing 13 g and having a Brinell hardness of 287 ± 8 , which is at least 60 points lower than that of any of the steel substrates used herein. Projectile velocities, determined with tandem chronographs, were varied by changing the quantity of gun powder (IMR 4895). The metric used for ballistic performance is V-50, the value for which there is a 50% probability of complete penetration of the target, calculated as the average of the lowest and highest velocities for complete penetration and partial penetration, respectively. For projectile speeds close to the V-50, both complete and partial penetrations may occur for apparently identical conditions. Complete penetration (sometimes referred to as the ballistic limit) required perforation of a 0.5 mm 2024 T3 aluminum witness plate located behind the target. The 30 cm \times 30 cm targets were mounted in a frame, with all shots falling at least 3 cm from the edge or any previous impact locus. Some ballistic results herein are reported after normalization by the V-50 of rolled homogeneous armor (RHA), a traditional steel for armor applications (Mil-DTL-12560).

The targets consisted of elastomer-coated substrates, the latter in some cases surface-hardened. Surface hardening methods included: electrolytic plating (Bales Mold Service, Inc.) with either chrome ("chromed") or chrome having dispersed diamond particles ("diamond chromed"), and vapor deposition (Sulzer Metco US, Inc.) of a carbon layer ("diamond-like carbon"). An elastomeric polyurea layer was added to the front (strike) face. The polyurea was prepared from Isonate 143L (Dow Chemical), a multifunctional methylene diphenylisocyanate, and Versalink P1000 (Air Products), a polytetramethylene oxide-di-p-amino-benzoate having a polydiamine with a molecular weight = 1000 g/mol; the components are mixed in a 1:4 ratio. Prior experiments showed comparable behavior for certain other elastomers (e.g. polyisobutylene), the key feature being a glass transition temperature such that the local segmental dynamics of the polymer transpire on the order of the impact frequency ($\sim 10^5$ s $^{-1}$) at the test temperature.^{3,5}

Brinell hardness measurements herein followed ASTM E10. Indentation experiments were used for surface-hardened plates; these employed a Hysitron BioIndenter (Hysitron Inc., Minneapolis, MN), with indents performed using a Berkovich indenter tip with

a nominal tip defect radius of 20 nm. Typically several dozen indents were measured per sample.

Digital image correlation (DIC) experiments, carried out at the Army Research Lab, were used to measure time-resolved deformations of targets subjected to impact below the ballistic limit.⁶ The instrument (GOM mbH of Braunschweig, Germany) employs two high-speed Phantom cameras to stereoscopically track the displacement of a fiducial pattern. Data were obtained every 6 μ s with a 2 mm spatial resolution. From these measurements, strains, velocities, and accelerations were obtained as a function of position relative to the impact locus.

Results

The spreading of the impact force due to the transient stiffening of the rubber coating can be inferred from the larger hole in penetrated substrates (Figure 1). A 25% increase in the area of the hole implies a proportional decrease in the initial impact pressure. (If the penetration mechanism involves shearing, this reduction in the pressure would be greater.) This change was sensibly independent of the thickness of either the substrate or the polyurea coating. To verify the consequent reduction in the impact pressure, strain measurements were obtained on the backside of coated and uncoated HHS plates (7.3 mm thick) using DIC. The projectile was a .50 cal fsp traveling 610 m/s, which is 35 m/s below the V-50 of the bare plate. Figure 2 shows the out-of-plane displacement at the target center and the in-plane displacement 8 mm away, respectively. For both the bare and coated HHS plate, there is a rapid rise in the deformation over the first 0.2 ms; this is consistent with the mean compressive strain rate, approximately 10^5 s $^{-1}$, calculated from the ratio of the projectile

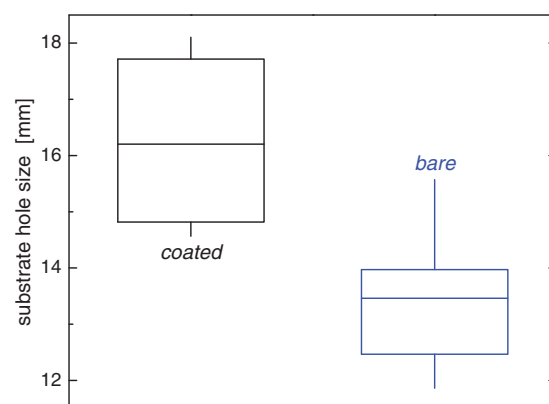


Figure 1. Box-and-whisker plot of hole size in HHS substrate after penetration by 0.50 cal fps with (left) and without (right) a front-side polyurea coating. Whisker ends represent one standard deviation above and below the mean.

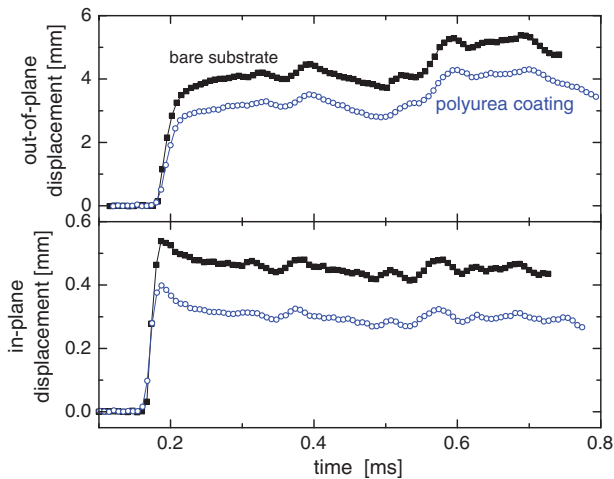


Figure 2. Displacements on backside of bare HHS (filled squares) and a bilayer of HHS and PU (open circles): (top) out-of-plane at the impact locus; (bottom) in-plane at a distance 8 mm from the impact.

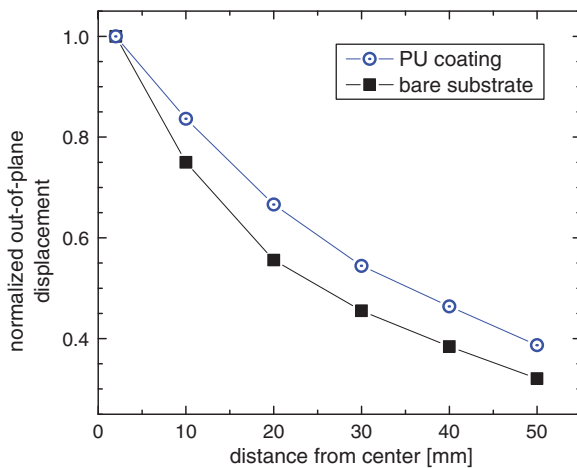


Figure 3. Maximum displacements on backside of bare HHS (filled squares) and a bilayer of HHS and PU (open circles) as a function of the distance from the impact locus. Note the ordinate values are normalized by the displacement at the impact center.

velocity and coating thickness. The in-plane displacement exhibits some recoil before attaining a permanent deformation; the latter is reduced by one-third when the polyurea coating is present. The out-of-plane deformation is reduced by about 20%. In Figure 3, the displacements (normalized by the maximum value at the impact center) are plotted as a function of distance from the impact. The coating spreads the strain laterally; that is, the perturbation decays over a broader distance, consistent with a larger substrate hole size for projectiles with sufficient velocity to penetrate the steel.

Collected in Figure 4 are ballistic results for polyurea/steel bilayers having various respective thicknesses

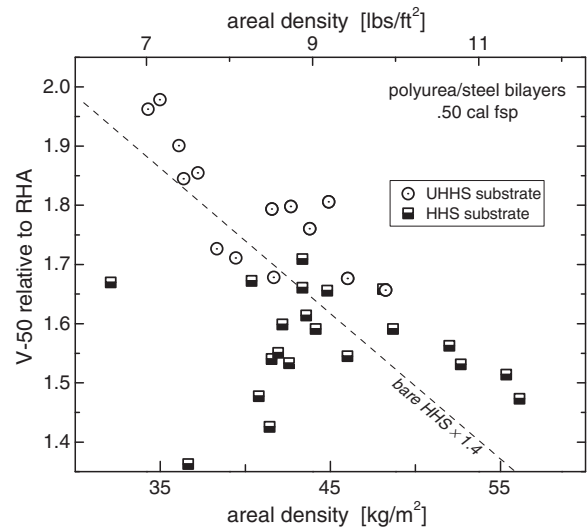


Figure 4. Comparison of ballistic performance of HHS and UHHS substrates with PU front-side coatings; ordinate is V-50 normalized by bare RHA steel of equal areal density (latter from MIL-DTL-12560). The rubber coatings were 1.5–14 mm thick, and the substrates had thicknesses varying over the range 3.7–5.3 mm. The dashed line represents the RHA-normalized V-50 of bare HHS (shifted up by a factor of 1.4 to bring them on scale with the bilayer data).

of coating and substrate. The data have been normalized to the V-50 of RHA. (The latter were taken from MIL-DTL-12560; these values are somewhat lower than the ballistic data for RHA reported by Gooch and Burkins.⁷) The thickness of both the steel and rubber were varied, to yield a broad range of weights and performance levels. The bilayers all perform better than bare RHA at equal areal density. The results in Figure 4 are for projectile-impact normal to the target (neglecting the minuscule deviation due to gyroscopic drift and precession of the rotating bullet.⁸) Normal incidence gives maximum compression of the coating and presumably the greatest contribution from the coating. For oblique incidence, the V-50 for the bilayer is larger; however, the increment due to the coating is significantly reduced (Table 1), reflecting attenuation of its rapid compression by the projectile.

One interesting aspect of the data in Figure 4 is that very generally, the performance is higher for coated UHHS than for the corresponding bilayers with HHS as the substrate. This is consistent with our previously reported finding that the substrate hardness enhances the contribution of the elastomer coating.⁵ The known mechanism for the ballistic enhancement, an impact-induced viscoelastic phase transition in the polymer with consequent large energy absorption and transient hardening of the coating,⁴ involves only the polymer; the function of the substrate is limited to enabling rapid compression of the coating. However, as seen in

Table 1. Diminution of coating effectiveness with projectile obliquity.

Angle	V-50 (m/s)		V-50 change due to coating
	Bare steel	Bilayer	
90°	600 ± 1	835 ± 9	39%
60°	745 ± 5	849 ± 2	14%
45°	823 ± 5	892 ± 7	8%

5.1 mm HHS; 1.5 mm thick polyurea.

Figure 4, the substrate material does affect the performance of the bilayer. We illustrate this more directly in Figure 5 (which includes some results from Roland et al.⁵). The upper panel shows V-50 measured for various metal substrates, having variations in both thickness and hardness (the latter from 90 to more than 600 on the Brinell scale). The correlation of the hardness of the bare metals with their ballistic performance is poor; from the value of the Pearson linear correlation coefficient, less than half the observed variance in V-50 can be ascribed to metal hardness.

These same substrates were then coated with the PU, and the ballistic penetration velocity measured. Plotted in the lower panel of Figure 5 is the difference between the V-50 for the coated and uncoated substrates; i.e. the increment in performance due to the polyurea. As seen, there is a strong dependence (correlation coefficient = 0.97) of the coating contribution on substrate hardness. Note that this is an effect of hardness, not substrate stiffness, as evidenced by the invariance of the V-50 increment to substrate thickness (data not shown).

The important performance metric, of course, is the net penetration resistance of the bilayer armor, which is not necessarily achieved by employing a harder substrate, even though this maximizes the coating contribution. For example, the V-50 of RHA increases by ~200 m/s by applying the PU, whereas that of UHHS increases by about 325 m/s. Nevertheless, in Figure 5 the performance of bare RHA is sufficiently higher than that of uncoated UHHS (due to the differences in plate thicknesses), that as a bilayer, the former yields a 20% higher V-50. This emphasizes that optimization of armor performance requires maximizing the coating contribution without loss of substrate properties. We illustrate a method to do this with a simple example. The steel plates prior to application of the coating are sand-blasted to remove rust and the surface layer of magnetite (Fe₃O₄). Removal increases the hardness of the surface layer by roughly 20 points on the Brinell scale. As shown in Table 2, there is a concomitant, albeit modest, increase in the V-50 after application of the coating. By comparison, for uncoated steel

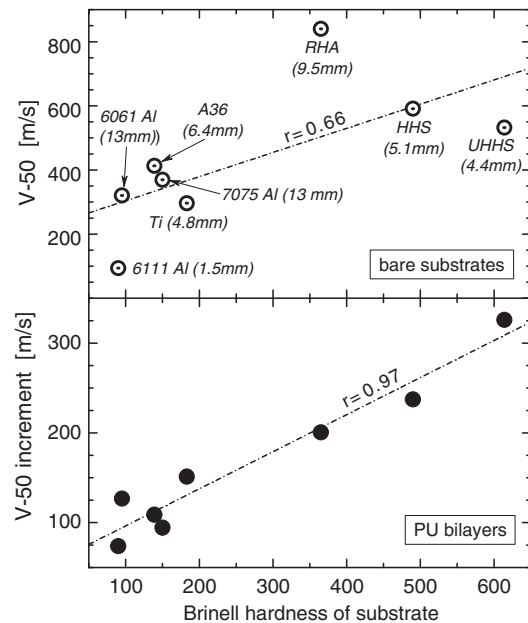


Figure 5. V-50 measured for (top) bare substrates of the indicated material and thickness; (bottom) the change in V-50 due to application of a 1.9 mm PU coating to the same substrates. Note that this V-50 increment is independent of the substrate thickness. Lines are the linear regressions, with the Pearson linear correlation coefficient indicated. Only for the bilayers is there a statistically significant correlation between performance enhancement and metal hardness. For the bare substrates the V-50 is not governed solely by the hardness; it is affected *inter alia* by the metal thickness.

Table 2. Effect of oxidized surface on ballistic performance.

Substrate	V-50 (m/s) ^c
Oxidized HHS ^a	834 ± 4
Sandblasted HHS ^a	839 ± 9
Oxidized UHHS ^b	850 ± 11
Sandblasted UHHS ^b	871 ± 4

^a5.1 mm thick.

^b5.3 mm thick.

^c2.8 mm PU thickness.

sand-blasting has a negligible effect on ballistic performance.

The changes in hardness and consequent increases in V-50 in Table 2 are barely significant, but the data serve to demonstrate the concept of surface-hardening to enhance the contribution of the polymer coating. To further pursue this approach, HHS steel plates were surface-treated to increase their hardness. A common method of surface-hardening steel is the application of a nitride coating. However, the nitriding process involves processing the steel at 400°C, which softens

HHS, resulting in deteriorated ballistic performance (Table 3).

For this reason, low temperature surface-hardening processes must be employed. Two coatings were applied to the steel using an electrolytic process, chrome and chrome containing diamond particles. In addition, a third coating was achieved by vapor deposition of carbon particles. From the load–displacement curves measured using nanoindentation,⁹ the plane-strain modulus and contact hardness were obtained for the untreated and untreated HHS; results are listed in Table 4.

Ballistic results for bilayers with surface-hardened HHS substrates are given in Table 5. There is a significant increase, approx. 8%, in V-50 for the two targets having substantially hardened substrates (more than a factor of two). The diamond-chrome coating, which yielded only a modest increase in substrate hardness (<10%), correspondingly showed a barely significant improvement in V-50. Note that the ballistic

performance of the bare steel was not measurably affected by surface-hardening (data not shown). The benefit of the harder substrate surface is to increase the V-50 increment conferred by the polyurea coating.

Discussion and summary

The presence of a few mm of elastomeric coating on the front surface of steel significantly increases the resistance to penetration by blunt steel projectiles. It is not an intuitive result that a soft polymer (Young's modulus $\approx 2\text{--}50$ MPa) would enhance the ballistic properties of armor, although two mechanisms have been established as contributing to the effect: energy absorption due to resonance between the polymer segmental dynamics and the impact frequency ($\approx 10^{-5}$ s), and lateral spreading of the force due to transient hardening of the coating. Although the data herein are for polyurea coatings, comparable results are obtained with other rubbers (e.g. polyisobutylene) that have a glass transition temperature sufficiently high that the segmental dynamics transpire on the time scale of the ballistic impact. Both mechanisms are a consequence of the rapid deformation of the coating, wherein the role of the underlying steel is merely to serve as a substrate that enables compression of the rubber. For this reason the elastomer bilayers offer less resistance to penetration by sharp ogives, such as AP bullets, which cut, rather than compress, the rubber coating. For such projectiles, it is necessary to first rotate or fracture the bullet, prior to its encounter with the coating. Ceramic elements have been found to be effective in this regard.^{10,11}

The results herein show an unexpected interaction between the coating and substrate, which we quantified from the increase in V-50 of the bilayer over that of the bare substrate. This estimate assumes no coupling of the coating and substrate, an assumption that can only be approximately true given the results in Figure 5 and Tables 2 and 5. Nevertheless, the main point is valid, that harder substrates allow better advantage to

Table 3. Effect of nitriding on ballistic performance of bare HHS (5.0 mm thickness).

	Brinell	V-50 (m/s)
Untreated	490	598 \pm 2
Nitride	415	433 \pm 3

Table 4. Nano-indentation results for surface-hardened HHS.

Surface treatment	Coating thickness (μm)	Modulus (GPa)	Hardness (GPa)
None	–	197 \pm 12	7.8 \pm 1.2
Diamond-like carbon	1.03 \pm 0.20	139 \pm 19	18.2 \pm 3.8
Chrome	3.81 \pm 0.09	267 \pm 30	18 \pm 4
Diamond chrome	3.58 \pm 0.14	197 \pm 25	8.5 \pm 1.5

Table 5. Ballistic results (2.8 mm polyurea coatings).

Substrate	Surface treatment	V-50 (m/s) ^a		
		Bare substrate ^b	PU-coated, untreated substrate	PU-coated, hardened-substrate
3.9 mm HHS	Diamond-like carbon	527 \pm 11	677 \pm 6	716 \pm 8 (6%)
4.4 mm HHS	Diamond-like carbon	535 \pm 4	743 \pm 7	800 \pm 5 (8%)
	Chrome			849 \pm 15 (8%)
4.7 mm HHS	Diamond chrome	550 \pm 8	788 \pm 4	807 \pm 11 (2%)

^a4.6 mm (0.180").

^bHardened and unhardened bare substrates have equivalent V-50.

be taken of the coating. The mechanism for this effect is unclear. The fact that thicker, and thus more rigid, substrates do not increase the coating contribution suggests the phenomenon arises from the mismatch of the layer impedances.^{12,13} This mismatch serves to spatially and temporally displace the incident shockwave, mitigating its impact on the substrate.

Any more rigorous analysis of the effect of substrate hardness suffers from the general difficulties encountered in theoretically modeling of hard armor incorporating soft polymers.^{14–17} Some success in describing the impact-induced viscoelastic transition has been reported,¹⁸ although the approach is largely empirical. The problem with such analyses^{19–26} is the complexity of the mechanical response of the coating. On impact, the polyurea exhibits (i) strong nonlinearity with an elastic regime followed by yielding; (ii) a sensitivity to both temperature (e.g. due to adiabatic heating) and pressure; (iii) extreme viscoelasticity (strain rate dependence of polymers is greatest in their glass transition regime); and (iv) a transient phase change accompanied by very substantial changes in mechanical properties. Thus, modeling efforts to date have been limited to either empirical descriptions that lack predictive capability, or more fundamental efforts that cannot address the myriad phenomena associated with the high strain, high strain rate response of elastomer-steel bilayers. Some limited efforts have been made to address interaction between the coating and substrate,^{27,28} but presently none have predicted the behavior reported herein. Other studies attempt to rationalize the behavior of the coatings under high strain rates and pressures in terms of the reorganization of the structure during shock loading.^{29–31} However, this cannot be the primary mechanism for the ballistic and blast properties of elastomeric coatings, since it has been shown that polymers having a homogeneous morphology perform equivalently.^{3,5}

Features of the ballistic properties of bilayers that require better understanding include: (i) the lateral dispersion in the impact force and its influence on penetration hole size (Figure 1); (ii) the mechanism giving rise to the effect of substrate hardness (Figure 5); (iii) the variation in V-50 with coating thickness, which shows a strong dependence for thin (< 2 mm) coatings, and a much weaker one for thicker coatings³; and (iv) the equivalence in performance of polyurea and butyl rubber coatings,^{3,5} contrary to interpretations of the behavior based on the unique properties of polyurea.^{29–31} Some efforts have addressed backside coatings,^{32,33} which are less effective than placement of the polymer on the strike-face side. Clearly more work is required to obtain a level of understanding sufficient for predictive capabilities in the design and optimization of elastomeric coatings for armor and impact-protective

barriers; notwithstanding, applications of this technology, both for military and civilian infrastructure protection are currently being pursued by ourselves and others.

Acknowledgements

We thank Joseph Lee and John Polesne of the Army Research Lab for carrying out the DIC measurements. CBG is grateful for an ASEE-NRL postdoctoral fellowship.

Declaration of Conflicting Interests

The author(s) declared no potential conflicts of interest with respect to the research, authorship, and/or publication of this article.

Funding

The author(s) disclosed receipt of the following financial support for the research, authorship, and/or publication of this article: This work was supported by the Office of Naval Research, in part by ONR Code 332 (R.G. Barsoum).

References

1. Matthews W. Polymer protection. *Technol Watch* April 26, 2004; p. 32.
2. Barsoum RGS and Dudt PJ. The fascinating behaviors of ordinary materials under dynamic conditions. *AMMTIAC Quart* 2010; 4: 11–14.
3. Roland CM, Fragiadakis D and Gamache RM. Elastomer-steel laminate armor. *Compos Struct* 2010; 92: 1059–1064.
4. Bogoslovov RB, Roland CM and Gamache RM. Impact-induced glass transition in elastomeric coatings. *Appl Phys Lett* 2011; 90: 221910.
5. Roland CM, Fragiadakis D, Gamache RM, et al. Factors influencing the ballistic impact resistance of elastomer-coated metal substrates. *Philos Mag* 2013; 93: 468–477.
6. Hisley DM, Gurganus JC and Drysdale AW. Experimental methodology using digital image correlation to assess ballistic helmet blunt trauma. *J Appl Mech* 2011; 78: 051022.
7. Gooch WA and Burking MS. Analysis of threat projectiles for protection of light tactical vehicles. In: *Proceedings of add-on armor conference*, Sterling Heights, MI, USA, 14–15 July 2004; reprinted by Army Research Lab, ARL-RP-89.
8. McCoy RL. *Modern exterior ballistics*, 2nd ed. Atglen, PA: Schiffer Publishing, 2012.
9. Oyen ML and Cook RF. A practical guide for analysis of nanoindentation data. *J Mech Behav Biomed Mater* 2009; 2: 396–407.
10. Walley SM. Historical review of high strain rate and shock properties of ceramics relevant to their application in armour. *Adv Appl Ceram* 2009; 109: 446–466.
11. Gooch WA. Overview of the development of ceramic armor technology: Past, present and the future. In: *35th international conference and exposition on advanced*

- ceramics and composites*, Daytona Beach, FL, USA, 23–28 January 2011.
12. Nesterenko VF. Shock (blast) mitigation by “soft” condensed matter. *MRS Symp Proc* 2003; 759MM4.3.1–4.3.12).
 13. Grujicic M, Yavari R, Snipes JS, et al. Molecular-level computational investigation of shock-wave mitigation capability of polyurea. *J Mater Sci* 2012; 47: 8197–8215.
 14. Amirkhizi AV, Isaacs J, McGee J, et al. An experimentally-based viscoelastic constitutive model for polyurea, including pressure and temperature effects. *Philos Mag* 2006; 86: 5847–5866.
 15. El Sayed T, Mock W, Mota A, et al. Computational assessment of ballistic impact on a high strength structural steel/polyurea composite plate. *Comput Mech* 2009; 43: 525–534.
 16. Chen C, Linzell DG, Alpman E, et al. Effectiveness of advanced coating system mitigating blast effect for steel components. *WIT Trans Built Environ* 2008; 98: 85–94.
 17. Amini MR, Amirkhizi AV and Nemat-Nasser S. Numerical modeling of response of monolithic and bilayer plates to impulsive loads. *Int J Impact Eng* 2010; 37: 90–102.
 18. Grujicic M, Pandurangan B, He T, et al. Computational investigation of impact energy absorption capability of polyurea coatings via deformation-induced glass transition. *Mater Sci Eng A* 2010; 527: 7741–7751.
 19. Chakkarapani V, Ravi-Chandar K and Liechti KM. Characterization of multiaxial constitutive properties of rubbery polymers. *J Eng Mater Technol* 2006; 128: 489–494.
 20. Roland CM and Casalini R. Effect of hydrostatic pressure on the viscoelastic response of polyurea. *Polymer* 2007; 48: 5747–5752.
 21. Choi T, Fragiadakis D, Roland CM, et al. Microstructure and segmental dynamics of polyurea under uniaxial deformation. *Macromolecules* 2012; 45: 3581–3589.
 22. Pathak JA, Twigg JN, Nugent KE, et al. Structure evolution in a polyurea segmented block copolymer because of mechanical deformation. *Macromolecules* 2008; 41: 7543–7548.
 23. Roland CM, Twigg JN, Vu Y, et al. High strain rate mechanical behavior of polyurea. *Polymer* 2007; 48: 574–578.
 24. Sarva SS, Deschanel S, Boyce MC, et al. Stress-strain behavior of a polyurea and a polyurethane from low to high strain rates. *Polymer* 2007; 48: 2213.
 25. Albrecht AB, Liechti KM and Ravi-Chandar K. Characterization of the transient response of polyurea. *Exp Mech* 2013; 53: 113–122.
 26. Holzworth K, Jia Z, Amirkhizi SV, et al. Effect of isocyanate content on thermal and mechanical properties of polyurea. *Polymer* 2013; 54: 3079–3085.
 27. Xue Z and Hutchinson JW. Neck development in metal/elastomer bilayers under dynamic stretchings. *Int J Solids Struct* 2008; 45: 3769–3778.
 28. Xue Z and Hutchinson JW. Neck retardation and enhanced energy absorption in metal–elastomer bilayers. *Mech Mater* 2007; 39: 473–487.
 29. Grujicic M, Pandurangan B, King AE, et al. Multi-length scale modeling and analysis of microstructure evolution and mechanical properties in polyurea. *J Mater Sci* 2011; 46: 1767–1779.
 30. Arman B, Reddy AS and Arya G. Viscoelastic properties and shock response of coarse-grained models of multi-block versus diblock copolymers: Insights into dissipative properties of polyurea. *Macromolecules* 2012; 45: 3247–3255.
 31. Grujicic M, Yavari R, Snipes JS, et al. Experimental and computational study of the shearing resistance of polyurea at high pressures and high strain rates. *J Mater Eng Perf* 2014; 24: 778–798.
 32. Xue L, Mock W and Belytschko T. Penetration of DH-36 steel plates with and without polyurea coating. *Mech Mater* 2010; 42: 981–1003.
 33. Amini MR, Isaacs JB and Nemat-Nasser S. Experimental investigation of response of monolithic and bilayer plates to impulsive loads. *Int J Impact Eng* 2010; 37: 82–89.